Optimisation of an Aeroelastic Flutter Energy Harvester

Leanne Grainger*†, Djamel Rezgui‡ and David Barton§
University of Bristol, Bristol, BS8 2BB, UK

This work is an investigation into approaches to optimising an aeroelastic flutter energy harvester in order to maximise power output. The flutter harvester was represented by a nonlinear two degree of freedom system coupled with a linear piezoelectric patch model. The energy harvester model was first optimised under steady state conditions and uniform flow speeds, to determine the values of tunable system parameters for which the power output is maximised. Parameters were then compared for their effectiveness and tuning ability. Furthermore, the performance of the harvester was also assessed at various flow distributions, since the uniform flow speed case is very idealistic. The assessment was carried out for different schemes for tuning the main system parameter for optimal energy generation. In these preliminary results the piezoelectric resistance was tuned to optimise the energy harvester and also used to test the tuning schemes. The three tuning schemes were; periodically setting the parameter, periodically sampling for a steady state before setting the parameter, and continuously varying the parameter.

Nomenclature

h	Heave displacement
α	Pitch angle
m_T	Flap and hinge mass
m_w	Flap mass
b	Flap semichord
x_α	Nondimensional distance between centre of mass and elastic axis
a	Position of elastic axis relative to semichord
d_h	Heave damping coefficient
d_α	Pitch damping coefficient
k_h	Heave stiffness
k_α	Pitch stiffness
$k_{\alpha 1}$	Quadratic nonlinear torsional stiffness coefficient
$k_{\alpha 2}$	Cubic nonlinear torsional stiffness coefficient
I_α	Moment of inertia about the elastic axis
θ	Piezoelectric coupling coefficient
V	Voltage
R	Resistance
C_p	Capacitance of the piezoelectric
L	Aerodynamic lift
M	Aerodynamic moment
a_0	Lift curve slope
ρ	Air density
U	Flow speed

*Correspondence to: leanne.grainger@bristol.ac.uk
†PhD student, Bristol Centre for Complexity Sciences.
‡Lecturer, Department of Aerospace Engineering.
§Lecturer, Department of Engineering Mathematics.

I. Introduction

Powering wireless sensors and electronics using piezoelectric energy harvesting has been an innovative approach to overcoming the problems of finite electrochemical batteries.[1–3] There are applications where a conventional battery would be disadvantageous, for example sensors in water systems or tracking tags on swimming or flying animals; in these applications the replacement of batteries would be impractical, expensive or impossible. Traditional piezoelectric energy harvesting has previously mainly focused on extracting energy from pre existing ambient vibrations.[4] However, a wider range of energy sources are now being considered as there are remote environments where there may not be a source of ambient vibrations, and it is in these locations that a battery independent solution is most needed. One energy source of interest is fluid flows, such as wind, to generate vibrations. While there has been research on harvesting energy from fluid-structure interaction, it is the flutter phenomenon that has proved most interesting.[5–7]

For many aeroelastic systems, there is a critical flow speed, known as the flutter speed, which defines the stability boundary for the system. Above this flutter speed, instability arises and the energy is being transferred from the fluid flow to the system and once the flow rate is large enough, self generated oscillations are produced in the form of limit cycle oscillations.[8]

An approach to harnessing this flutter phenomenon using an aeroelastic flutter energy harvester was first proposed by Bryant and Garcia.[9] An example of such a device is a simple cantilevered piezoelectric beam and a pin connected flap that can be driven by flow speeds above the flutter boundary to produce energy.

The optimisation of a single aeroelastic flutter energy harvester requires consideration of structural, fluid and electrical dynamics. This is complicated further as such an energy harvester is required to work across a wide range of operating conditions. There has been much investigation into optimising the system parameters to minimise the critical flutter speed as to optimise the range of flow speed the energy harvester can operate within.[10] As well as improving the the range of operational flow speeds, it is also desirable to enhance the system to maximise the power output. This type of energy harvester currently doesn't generate much power, milliwatts are produced intended to power small sensor systems rather than contribute to the grid. Therefore it is advantageous to maximise the energy yield as much as possible.

One approach to maximise the power output of an energy harvester would be to alter certain parameters during operation such that, for the current flow conditions, optimal energy is generated. By testing each parameter that can be tuned, it can be determined which would be most effective and therefore most worthwhile to implement. Candidate tuning parameters and their effectiveness will be found by using a model of a flutter energy harvester and comparing the power output across a range of flow speeds for a range of tuning parameter values. These results alone will not be enough to conclude how effective tuning a parameter will be at maximising the energy yield of a harvester. This is due to the variety of potential flow distributions that the harvester could be subjected to when in operation. Therefore different tuning schemes will be investigated for various flow distributions.

II. Method

A. System Model

The system that will be modelled is that of a two degree of freedom flutter energy harvester. Although this work will not focus on a specific design, to give an example, a generic flutter energy harvester consists of a wing-like flap at the end of a flexible beam. The flap is connected to the beam by a hinge, and the beam has piezoelectric patches along either, or sometimes both, of its sides. Diagrams of an example of the harvester design and the harvester schematics are shown in Figure 1. The degrees of freedom are the displacement of the beam, referred to as the heave (h), and the angle of the rotation of the flap, known as the pitch (α). The system is electromechanically coupled to include the piezoelectric transduction. The model equations are

$$m_T\ddot{h} + m_w x_\alpha b\ddot{\alpha} + d_h\dot{h} + k_h h = L - \theta V, \tag{1}$$

$$m_w x_\alpha b\ddot{h} + I_\alpha\ddot{\alpha} + d_\alpha\dot{\alpha} + k_\alpha(\alpha)\alpha = M, \tag{2}$$

$$\frac{V}{R} + C_p\dot{V} - \theta\dot{h} = 0, \tag{3}$$

where m_T is the tip mass, m_w is the mass of the flap, x_α is the nondimensional distance between centre of gravity and elastic axis of the wing, b is the semichord of the flap, d_h is the damping coefficient for heave, d_α is the damping coefficient for pitch, k_h is the heave stiffness, $k_\alpha(\alpha)$ is the pitch stiffness and I_α is the moment of inertia about the elastic axis. V is the voltage, R is the resistive load, θ is the piezoelectric coupling coefficient[11] and C_p is the capacitance of the piezoelectric.

This models the beam of the energy harvester having a piezoelectric strip along one side, when there is heave motion the piezoelectric is stretched or compressed and a voltage V is generated. The current model assumes that the piezoelectric beam only undergoes one bending mode. Including the effects of all other possible bending modes would mean that the other energies that could be generated by the modes can also be observed. Including more than one bending mode will be considered in future work.

The source of nonlinearity in this system is the concentrated pitch nonlinearity, modelled by quadratic and cubic terms in the torsional spring,

$$k_\alpha(\alpha) = k_{\alpha 0} + k_{\alpha 1}\alpha + k_{\alpha 2}\alpha^2. \tag{4}$$

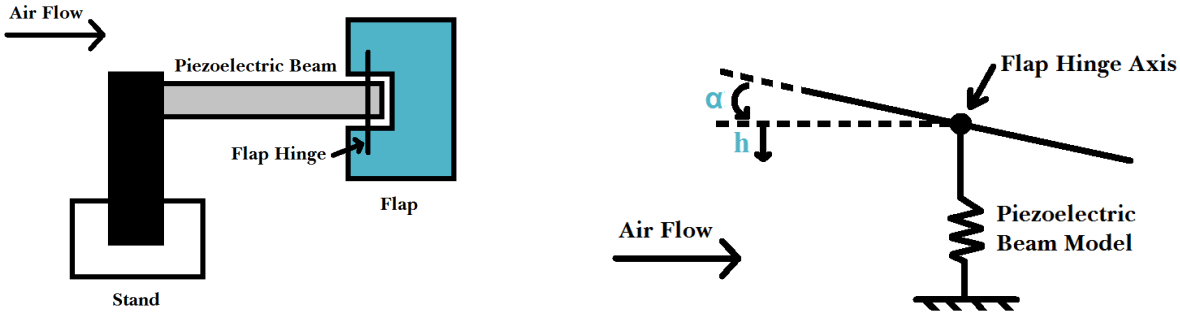

(a) (b)

Figure 1. (a) is an example of an aeroelastic flutter energy harvester design. The flap rotates from side to side (in and out of the page) about the flap hinge and the piezoelectric beam bends from side to side which generates energy. (b) is an aeroelastic flutter energy harvester schematic with the degrees of freedom shown: angle of flap (α) and displacement of beam (h).

A quasi steady approximation of the aerodynamics was used to create a simple model of an energy harvester. Although this type of model is less accurate and gives a higher flutter speed when compared to experimental results than unsteady models such as Duhamel formulation,[7] the quasi steady model was used to obtain preliminary results more quickly. However, later in this work an unsteady model of the aerodynamics will be implemented.

The quasi steady aerodynamic forces are represented by the aerodynamic lift and moment about the elastic axis as derived by Theodorsen[12] in incompressible flow, denoted by L and M, respectively.

$$L = -\frac{a_0}{2}\rho b^2\left[\ddot{h} + U\dot{\alpha} - ba\ddot{\alpha}\right] - a_0\rho UbQ, \tag{5}$$

$$M = \frac{a_0}{2}\rho b^2\left[ba\ddot{h} - Ub\left(\frac{1}{2} - a\right)\dot{\alpha} - b^2\left(\frac{1}{8} + a^2\right)\ddot{\alpha}\right] + a_0\rho Ub^2\left(a + \frac{1}{2}\right)Q, \tag{6}$$

where

$$Q = U\alpha + \dot{h} + \dot{\alpha}b\left(\frac{1}{2} - a\right). \tag{7}$$

In these equations U is the flow speed and a_0 is the lift curve slope.

B. Parameter Assessment to Harvested Energy

Given the conditions of a uniform flow speed and some system parameters as they are, what can be done to optimise the power output will be investigated. The flutter energy harvester model will initially be tested with steady state conditions. The optimisation will be done by finding the values of system parameters for which the power output is maximum. This will be carried out for a realistic range of flow speeds. The system parameters to be optimised are ones that we can change, which includes the piezoelectric resistance and the nonlinear torsional spring coefficients. The current values of the optimal resistances across wind speed are only approximations. In further work the approximations will be made more accurate by running the model over a wider ranges of parameter values and wind speeds in order to have a more complete data set.

These optimal values are approximated by running the model over a range of parameter values, for a range of flow speeds above the flutter speed. For each flow speed, the value which corresponds to the maximum power output is stored. The energy harvested is calculated using $P = IV$, where $I = \frac{V}{R}$ is the current, and it is the root mean square (rms) power per second over one oscillation that is used.

C. Tuning Schemes

For the static case, where the flow speed is uniform and the system is in a steady state, the tuned system parameter can simply be set at its optimal value. However, the environment in which a harvester will be used will not be static, but will be continuously varying. Therefore, a way to tune a system parameter to its optimum as the flow conditions change is needed. There are several ways of varying the chosen tuning parameter to the most optimal value as the flow conditions change. Here are some possible tuning schemes:

A. periodically setting the resistance,

B. periodically sampling, waiting for a steady state then setting the resistance, and

C. continuously varying the resistance.

In order to facilitate continuously varying the resistance, the relationship between the optimal resistance and the voltage was approximated using a fourth order polynomial curve fitting, as shown in figure 2.

The optimal resistance, R_{opt}, as a function of the voltage, V, was expressed by the equation:

$$R_{opt}(V) = -0.014309V^4 + 3.5242V^3 - 278.83V^2 + (7.1605 \times 10^3)V + 6.12 \times 10^5 \tag{8}$$

A comparison will be made between the schemes as well as to the model without tuning, where the parameter will be kept constant at a mean of its optimal values.

The tuning schemes were compared to only one fixed resistance. However, comparing the tuning schemes to the system set at other fixed parameter values will broaden our understanding of the effect of the three tuning schemes and will be carried out in further testing.

In order to set the parameter, all three schemes need to determine the current flow conditions so that the corresponding optimal parameter can be tuned to. The voltage output is used as an indicator of the flow conditions and therefore which parameter value the energy harvester should be tuned to. This process requires energy, and as each scheme does this a different number of times, each scheme will require different amounts of energy to implement.

The second tuning scheme in the list is the only one to involve sampling for a steady state. Ideally, the system needs to be in a steady state in order to tune accurately. When there is a change in the conditions that the energy harvester is under, for example a change in flow speed, or when the initial conditions are far from conditions in a steady state, the system experiences a transient state. The oscillations of the system increase or decrease in amplitude, until a steady state is reached, at which point the oscillations stop or the oscillations continue with near constant amplitude. It would be unfavourable to tune a parameter during the transient state, before the system has settled into a steady state, because the value that the system parameter will be tuned to will not correspond to the actual flow conditions. Although sampling will cost energy, it will also mean that the parameter will be set when there are the best conditions for the parameter to be tuned accurately. On the other hand, the likely disadvantage of this scheme is that it is possible for the system to rarely reach a steady state if the flow conditions change very often.

The scheme most likely to give the best results is that of continuously varying the parameter to its optimal value. The drawback of this scheme is that it is the most energy expensive. However, by continuously checking

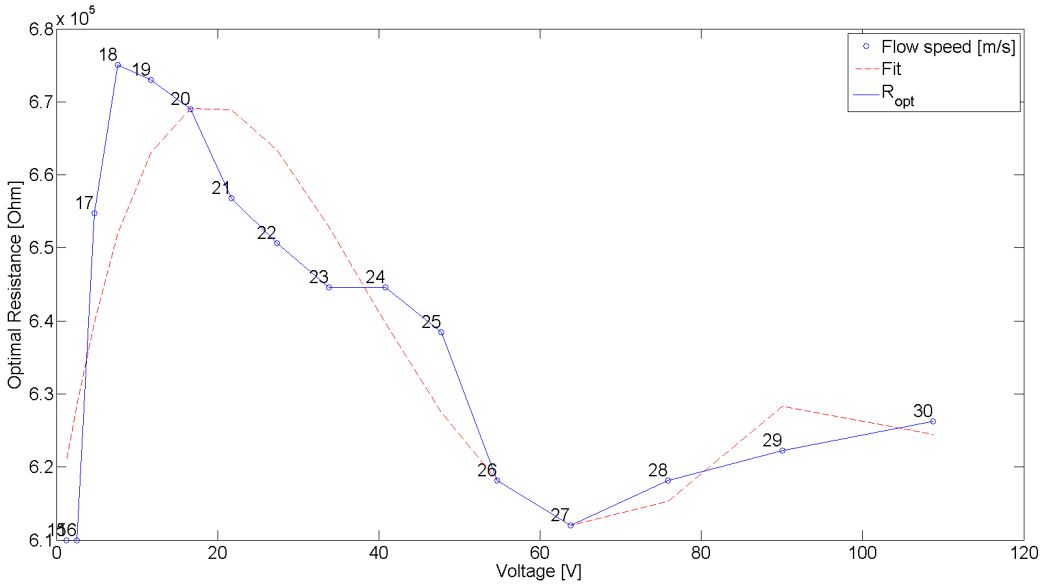

Figure 2. The optimal resistance against filtered voltage. The line labelled R_{opt} shows how the optimal resistance varies with voltage. The points marked along the line are the data points and are labelled with the corresponding flow speed. The line labelled Fit, is a fourth order polynomial curve fitting, used in tuning scheme C to continuously vary the resistance.

the current flow conditions and varying the parameter accordingly, the system is likely to be kept at, or close to, maximum power generation.

The first tuning scheme of periodically setting the parameter is the least likely to be effective at optimising the harvester as it has the potential to be delayed in setting the optimal parameter for the current flow conditions. However, this scheme requires the least energy to implement of the three schemes which is desirable and it could be a compromise between the two other schemes.

To further this study, an analysis across a larger dataset, considering more operating conditions and parameter values will be carried out. With more data to examine, a better interpretation of the effect of tuning system parameters in different ways on maximising the power can be made.

D. Wind Distribution

The conditions that a flutter energy harvester will experience will not be uniform and in a steady state as for the first optimisation to be carried out with the model. The conditions will be very variable, and so to test the model and the tuning schemes other flow conditions will be considered. They will be:

- uniform flow speed,
- ramp flow distribution, where the flow speed increases from zero until it reaches a certain flow speed and then becomes uniform, example shown in figure 3, and
- realistic flow distribution, modelled by a summation of sine waves using amplitudes and frequencies of experimental data of wind distributions,[13] example shown in figure 3.

The realistic wind speed, U, is modelled as a function of time, t, using the following equation:

$$U(t) = \Sigma_i A_i \sin(\omega_i t + \varphi_i) + \beta \tag{9}$$

where A is the amplitude, ω is the frequency, φ is the phase and β is the offset. We set $i = 3$, with $A_{1,2,3} = 3$, $\omega_1 = 0.1$, $\omega_2 = 0.15$ and $\omega_3 = 0.25$. Stochasticity is introduced as the φ_i values are set randomly between 0 and 2π. Values of 15 and 25 are used for β, which determines the overall average flow speed.

Uniform flow speed is the simplest case examined, giving the opportunity to look at how the system reacts to a specific flow speed. Flow speed being uniform for a long period of time is an extreme case in terms of realistic flow distribution an energy harvester might usually experience, but would be possible to recreate experimentally and would be useful to verify the model.

The case of a ramp flow distribution is more complex than the uniform flow speed, but is still an extreme example of wind distribution. This ramp wind distribution is representative of wind speed steadily increasing from zero wind speed, meaning it is continuously changing, contrasting with what we saw with the uniform wind speed.

The stochastic wind distribution is intended to be a approximation of what a realistic wind distribution would be in reality. Of the three distributions this could provide the most informative results as it will be the closest approximation of the kind of wind distribution a flutter harvester would experience.

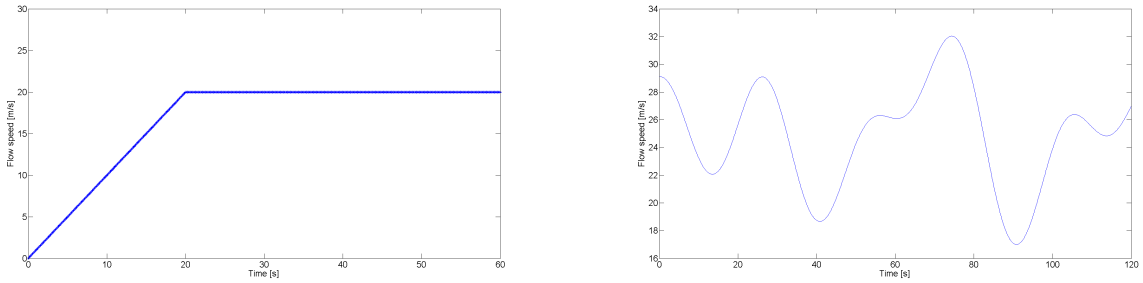

(a) (b)

Figure 3. (a) is an example of a ramp wind distribution. The wind speed increases from 0 to 20 m/s over 20 seconds, then continues at a uniform flow speed. (b) is an example of a realistic wind distribution, with an overall average wind speed of 25 m/s.

III. Results

A. Optimising Energy Harvester Parameters

Preliminary results have been carried out for optimising resistance. The rms power was found for a range of flow speeds for different values of resistance. We can see in figure 4, that there is an optimal resistance that occurs at a certain value of R across the flow speeds, at which there is maximum power output. However, across wind speed, the optimal range of resistances is not very wide. Although this means that tuning the resistance will not result in much of a power gain, there is a sufficient enough difference to use this parameter to obtain preliminary results.

The effect of changing the cubic coefficient of the nonlinear torsional spring, $k_{\alpha 2}$, on power output has also started to be investigated. This was done while the ranges of resistance were estimated, which also gave insight into the effect of $k_{\alpha 2}$ on optimal resistance.

For $k_{\alpha 2} = 107$ N m, shown in figure A, we see that the optimal resistances range from 0.58 to 0.7 $M\Omega$. For $k_{\alpha 2} = 10.7$ N m, shown in figure A, the optimal resistances range from 0.64 to 0.7 $M\Omega$ and for $k_{\alpha 2} = 3.21$ N m, shown in figure A, the range is between 0.67 and 0.73 $M\Omega$. From this we can see that changing the value of $k_{\alpha 2}$ does not increase the range of optimal resistances, but decreases the range.

From this data we can also see the effect of changing $k_{\alpha 2}$ on the power output across the flow speeds. For $k_{\alpha 2} = 107$ N m, this ranges from 0.001 to 0.3 mW. For $k_{\alpha 2} = 10.7$ N m, the range was 0.001 to 0.007 W and for $k_{\alpha 2} = 3.21$ N m, it was between 0.018 to 0.07 W. We can see that as $k_{\alpha 2}$ decreases, the power output increases.

Other system parameters will be tested in the future for their effectiveness on optimising power output. Meanwhile, preliminary results have been carried out for tuning resistance in the tuning schemes proposed.

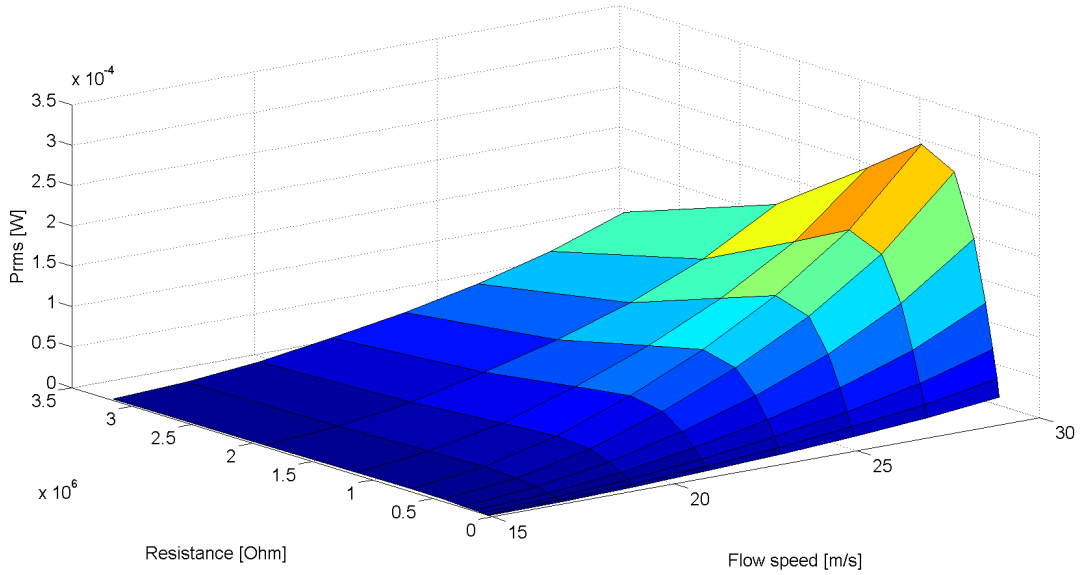

Figure 4. The variation of the root mean square (rms) power per second with resistance and flow speed. The rms power increases with the flow speed. The rms power increases and then decreases with resistance.

Tuning Scheme	Description
None	No tuning; resistance is kept constant
A 5	Periodically setting the resistance every 5 seconds
A 10	Periodically setting the resistance every 10 seconds
A 15	Periodically setting the resistance every 15 seconds
B 5	Periodically checking for a steady state then setting the resistance every 5 seconds
B 10	Periodically checking for a steady state then setting the resistance every 10 seconds
B 15	Periodically checking for a steady state then setting the resistance every 15 seconds
C	Continuously varying the resistance

Table 1. Table of the descriptions of each tuning scheme and the terms used to refer to them.

B. Comparison of Tuning Schemes

1. Uniform wind distribution

The tuning schemes are first compared for the uniform flow speed case. The results found are shown in figure 6. They show the average power output per second for each of the tuning schemes for uniform flow speeds of 15 m/s, 20 m/s and 25 m/s. The height of the bars represents the average power output per second, which was calculated after running the model for 120 seconds. There are eight tuning schemes in total for this type wind distribution, corresponding to each bar in the graph. This is because the periodic tuning schemes are tested for three different time intervals. The tuning schemes are listed in Table 1.

If we first compare the two periodic tuning schemes, A and B, we can see that tuning scheme B is more effective at tuning the harvester to obtain more power than tuning scheme A across the three wind speeds tested. This suggests that for uniform wind speeds, periodically sampling the voltage and waiting for a steady state to be reached before setting the resistance is more favourable than periodically setting the resistance regardless of whether or not a steady state has been reached. This most likely arises from the fact that by waiting for the steady state to be reached, the desired optimal resistance is tuned more accurately. If the system is in a transient state, it is more likely that an undesirable resistance will be chosen.

For both tuning schemes A and B, the results suggest that the shortest period may be the least effective,

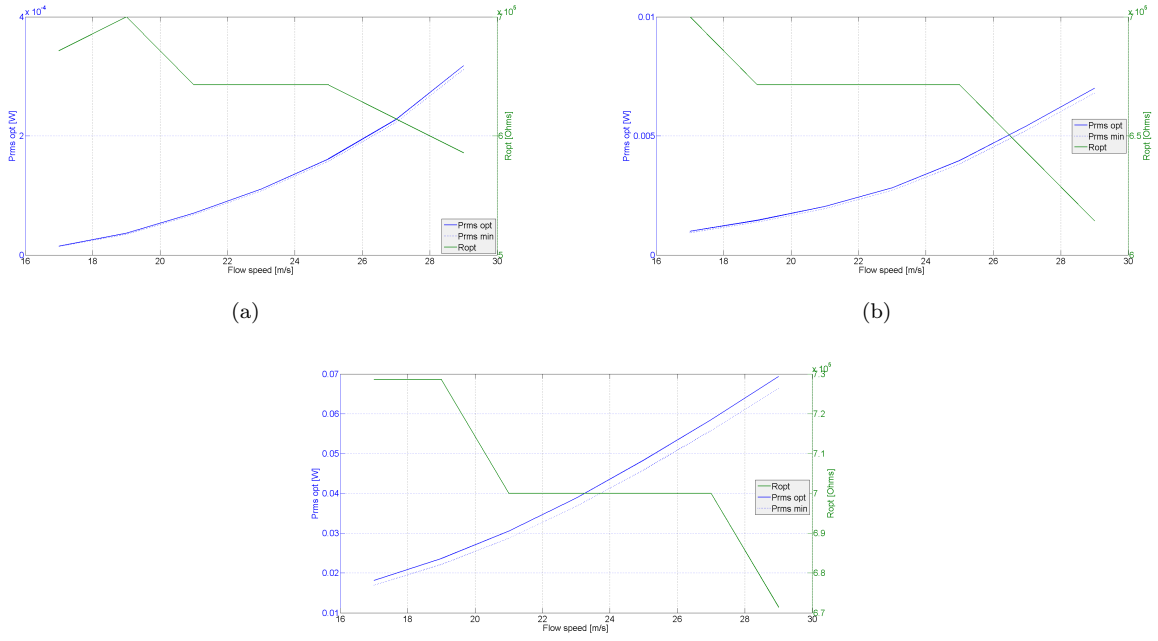

(a) (b)

(c)

Figure 5. The variation of the optimal root mean squared power output, P_{rms} opt, the minimum root mean squared power output, P_{rms} min, and the optimal resistance, R_{opt}. This is for three values of the coefficient of nonlinear torsional spring, $k_{\alpha 2}$: (a) 107 N m, (b) 10.7 N m and (c) 3.21 N m.

particularly for the results for 15 m/s. This may be due to the nature of the transient of lower wind speeds, as perhaps the error used to decide when a steady state is reached isn't low enough to correctly detect a steady state after a short period of time. Using a longer time interval may also mean that a steady state is more likely to have been reached, resulting in more accurate tuning. However, as the difference between all of these average power outputs that are being compared is very small it is difficult to say.

Comparing tuning scheme C, continuously varying the resistance, to using no tuning scheme at all it can be seen that not tuning at all is better for more power generation for wind speeds of 15 and 25 m/s but continuously varying the resistance is better for the wind speed of 20 m/s. Not tuning the resistance is most likely more effective than continuously varying the resistance due to the inaccuracy of the equation used for continuously varying the resistance. This suggests that finding a more exact equation for the optimal resistance as a function of voltage would be a more reasonable tuning scheme, however, the one used for these preliminary results may be too far from optimal to be effective across many wind speeds.

Comparing all tuning schemes, it can be said that tuning scheme B with a time interval of 15 seconds is consistently better than all other tuning schemes for uniform wind distribution.

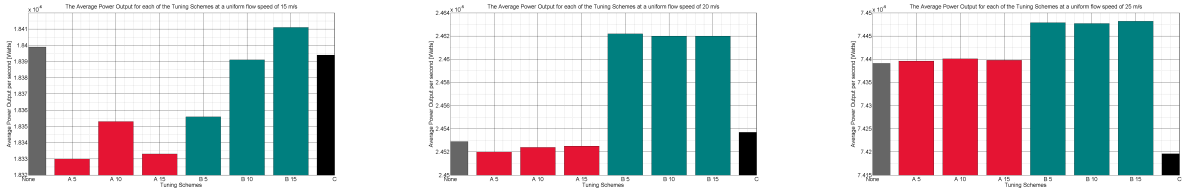

(a) (b) (c)

Figure 6. The average power output per second for each of the tuning schemes for uniform flow speeds of (a) 15 m/s, (b) 20 m/s and (c) 25 m/s. The height of the bars represents the average power output per second. The bars correspond to the tuning schemes that are listed in Table 1.

2. *Ramp wind distribution*

The tuning schemes are also compared for the ramp wind distributions. The results found are shown in figure 7. They show the average power output per second for each of the tuning schemes for ramps of 10 and 20 seconds in length, each reaching uniform flow speeds of 15 m/s, 20 m/s and 25 m/s. The height of the bars represents the average power output per second, which was calculated after running the model for the length of the ramp. There are four tuning schemes in total for this type wind distribution, which correspond to each bar in the graph. This is because the periodic tuning schemes are tested for only one time interval of 5 seconds. The tuning schemes are listed in Table 1. However, schemes A 10, A 15, B 10 and B 15 are not included in this wind distribution. This is due to the ramp lengths being 10 and 20 seconds long, meaning that these schemes with longer periods cannot tune during the ramp length.

Comparing the periodic schemes for both ramp lengths, A is more optimal than B for 15 and 20 m/s, but B is better than A for 25 m/s. This may be because there are likely to only be one or few steady states detected during the ramp as the wind speed is constantly changing. Therefore tuning with B means that tuning isn't occurring, even though as indicated by A, it could be worth tuning during the ramp even if a steady state isn't reached. For the case of 25 m/s it may be that if steady states were reached then B is more capable of choosing the most optimal resistance for the system as it is using the voltage at the detected steady state to decide on the new resistance, whereas A uses the last detected voltage of the 5 second interval which may not be indicative of what will be optimal for the next 5 seconds.

The results show that continuously tuning the resistance rather than keeping the resistance constant, is always more advantageous. This tuning scheme is also shown to be the optimal tuning scheme in 5 out of 6 of the cases. This suggests that during a dramatic change in flow speed, continuously changing the resistance is the most capable scheme. Our equation for optimal resistance as a function of voltage must be a close fit for the range of voltages produced during this type of wind distribution.

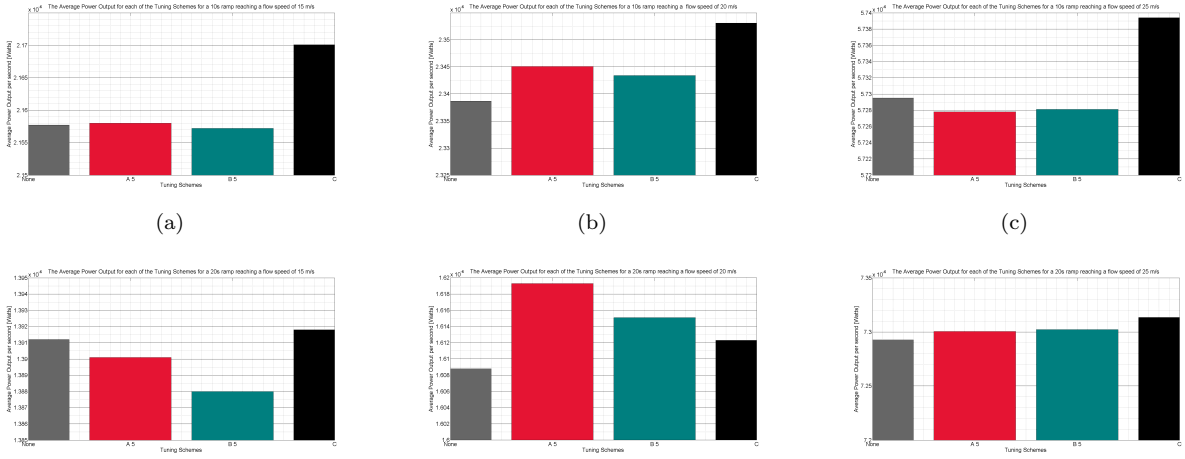

Figure 7. The average power output per second for each of the tuning schemes for ramps of 10 seconds in length: (a), (b), (c) and 20 seconds in length: (d), (e), (f). Each ramp reaching uniform flow speeds of 15 m/s: (a), (d), 20 m/s: (b), (e) and 25 m/s: (c), (f). The height of the bars represents the average power output per second. The bars correspond to the tuning schemes that are listed in Table 1 excluding A 10, A 15, B 10 and B 15.

3. *Realistic wind distribution*

Finally the tuning schemes are compared for the realistic wind distributions. The results are shown in figure 8. They show the average power output per second for each of the tuning schemes for realistic flow distributions of overall average flow speeds of 15 m/s and 25 m/s. The height of the bars represents the average power output per second, which was calculated after running the model for 120 seconds. There are eight tuning schemes in total for this type wind distribution, corresponding to each bar in the graph. This is because the periodic tuning schemes are tested for three different time intervals. The tuning schemes are listed in Table 1.

Between tuning schemes A and B, A seems to be the more effective. However, comparing the time intervals in each tuning scheme, A 5 and B 10 are better for both flow distributions., but between A 15 and B 15 it is unclear.

Using no tuning scheme, keeping the resistance fixed at 0.6 $M\Omega$, is the optimal strategy for the the flow distribution with an average wind speed of 15 m/s. As this value is close to the optimal resistance for 15 m/s, 0.61 $M\Omega$, not tuning appears to mean that this fixed resistance is optimal for the majority of flow speeds and the transients that occur between. As 0.6 $M\Omega$ is not close to the optimal resistance for a flow speed of 25 m/s, keeping the system fixed at this resistance while it's experiencing flow speeds around 25 m/s, means that the resulting average output is one of the lowest compared to the tuning schemes. However, if the fixed resistance was closer to the optimal for 25 m/s, we may have also found that not tuning would be the optimal strategy for this wind distribution. Then again, it is important to remember that the flutter speed for this system is 15 m/s, and so the first flow distribution will include some flow speeds for which the harvester cannot generate energy, which might influence how that compares to a higher flow distribution.

Of the three tuning schemes, A 5 results in the highest power output in both cases, B 10 coming in a close second.

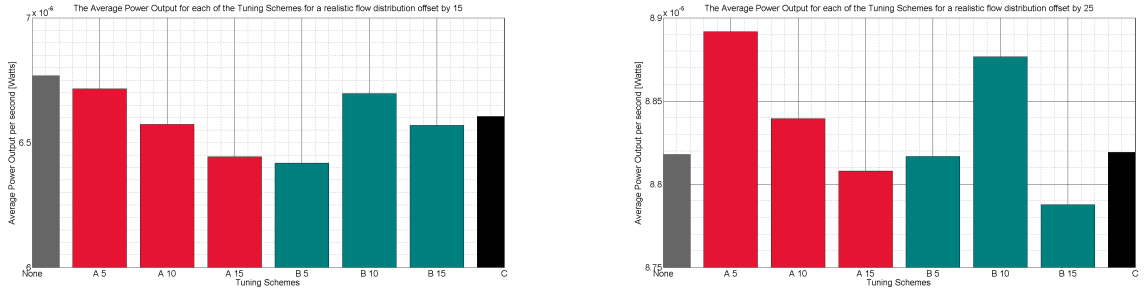

(a) (b)

Figure 8. The average power output per second for each of the tuning schemes for realistic flow distributions of average flow speeds of (a) 15 m/s and (b) 25 m/s. The height of the bars represents the average power output per second. The bars correspond to the tuning schemes that are listed in Table 1.

IV. Conclusion

From this preliminary study there was no consensus between the wind distributions investigated on which tuning scheme is optimal for maximising power output by tuning resistance. For a uniform wind distribution it was found that periodically checking for a steady state then setting the resistance was the most effective scheme for maximum power output. Continuously varying the resistance was the best strategy for the majority of cases when looking at the ramp wind distribution, whereas periodically setting the resistance was the most effective in most cases for the realistic wind distribution. However, it is a promising indication that tuning a flutter energy harvester for maximal power output is possible and worth implementing. With further work carried out on this model, using more data that is more accurate to explore the questions that this work has raised so far, it will be possible to affirm an optimal tuning strategy.

Future work will be focused on optimising a refined aeroelastic flutter energy harvester model with other system parameters, as well as resistance, both in steady state conditions and varying flow conditions. The energy increase by tuning the resistance for the harvester in this model is very small, and therefore finding other more effective parameters will be important.

Next steps include using numerical continuation methods for bifurcation analysis of the system and for calculations of the power output as well as investigating more real wind distribution data and other methods of simulating realistic wind distributions.

References

[1]H. A. Sodano, D. J. Inman, and G. Park, "A review of power harvesting from vibration using piezoelectric materials," *Shock and Vibration Digest*, vol. 36, no. 3, pp. 197–206, 2004.

[2]S. P. Beeby, M. J. Tudor, and N. White, "Energy harvesting vibration sources for microsystems applications," *Measurement science and technology*, vol. 17, no. 12, p. R175, 2006.

[3]D. Guyomar and M. Lallart, "Recent progress in piezoelectric conversion and energy harvesting using nonlinear electronic interfaces and issues in small scale implementation," *Micromachines*, vol. 2, no. 2, pp. 274–294, 2011.

[4]S. R. Anton and H. A. Sodano, "A review of power harvesting using piezoelectric materials (2003–2006)," *Smart materials and Structures*, vol. 16, no. 3, p. R1, 2007.

[5]M. Bryant, R. L. Mahtani, and E. Garcia, "Wake synergies enhance performance in aeroelastic vibration energy harvesting," *Journal of Intelligent Material Systems and Structures*, vol. 23, no. 10, pp. 1131–1141, 2012.

[6]M. Bryant, E. Wolff, and E. Garcia, "Parametric design study of an aeroelastic flutter energy harvester," in *SPIE Smart Structures and Materials+ Nondestructive Evaluation and Health Monitoring*, pp. 79770S–79770S, International Society for Optics and Photonics, 2011.

[7]A. Abdelkefi, R. Vasconcellos, A. H. Nayfeh, M. R. Hajj, and O. Badran, "Nonlinear analysis and identification of limit cycle oscillations in an aeroelastic system," in *53rd AIAA/ASME/ASCE/AHS/ASC Structures, Structural Dynamics and Materials Conference 20th AIAA/ASME/AHS Adaptive Structures Conference 14th AIAA*, 2012.

[8]D. H. Hodges and G. A. Pierce, *Introduction to structural dynamics and aeroelasticity*, vol. 15. cambridge university press, 2011.

[9]M. Bryant and E. Garcia, "Modeling and testing of a novel aeroelastic flutter energy harvester," *Journal of vibration and acoustics*, vol. 133, no. 1, p. 011010, 2011.

[10]M. Bryant, E. Wolff, and E. Garcia, "Aeroelastic flutter energy harvester design: the sensitivity of the driving instability to system parameters," *Smart Materials and Structures*, vol. 20, no. 12, p. 125017, 2011.

[11]A. Erturk and D. J. Inman, "A distributed parameter electromechanical model for cantilevered piezoelectric energy harvesters," *Journal of Vibration and Acoustics*, vol. 130, no. 4, p. 041002, 2008.

[12]T. Theodorsen, "General theory of aerodynamic instability and the mechanism of flutter," 1949.

[13]I. Van der Hoven, "Power spectrum of horizontal wind speed in the frequency range from 0.0007 to 900 cycles per hour," *Journal of Meteorology*, vol. 14, no. 2, pp. 160–164, 1957.